The dynamical dimension of defects in spatiotemporal chaos

David A. Egolf
Laboratory of Atomic and Solid State Physics, Cornell University, Ithaca, NY 14853-2501
(December 6, 1997)

Using a new time-dependent measure, we demonstrate for the first time that each defect in a representative defect-mediated spatiotemporally chaotic system is associated with one to two degrees of dynamical freedom. Furthermore, we show that not all dynamical degrees of freedom are related to the defects; additional degrees of freedom are due to underlying phase turbulence. These results yield a deeper understanding of the dynamical role of defects and provide hope that these complicated systems might be reduced to simpler descriptions.

05.45.+b, 47.52.+j, 47.54.+r

I. INTRODUCTION

The motions and interactions of topological defects dominate, at least visually, the dynamics of a wide variety of nonequilibrium systems [1]. This behavior is observed in systems as diverse as chemical reactions in shallow layers (e.g., [2]), thermal convection in horizontal fluid layers (e.g., [3]), aggregation in slime mold colonies (e.g., [4]), periodically shaken layers of sand (e.g., [5]), and electrical activity waves in heart tissue (e.g., [6]). Researchers have proposed that the macroscopic behavior of these complicated systems can be understood by considering a simpler system of interacting defects [1], instead of the detailed equations describing the system.

Some nonequilibrium systems containing defects are also spatiotemporally chaotic, in that the spatially and temporally disordered dynamics continues indefinitely. These systems are often termed "defect-mediated" to emphasize the role of the defects. For such systems one might intuitively expect that a measure of the average complexity D of the system (roughly the minimum number of degrees of freedom to describe the dynamics) is proportional to the average number of defects $\langle n_d(t)\rangle_t$ in the system. More generally, we consider the possibility of a contribution unrelated to the defects, and we account for the time-dependence of the quantities:

$$D(t) = D_b(t) + D_d\, n(t), \tag{1}$$

where D_d is the average contribution per defect. The background term $D_b(t)$ is expected to be non-zero if the field between the defects does not simply respond passively to the motion of the defects.

Eq. (1) is important to understand for several reasons. First, insight will be gained into what drives the dynamics of defect-mediated chaotic systems; i.e., whether the defects alone determine the dynamics. This result may be an important step toward understanding not only the building blocks of extensive chaos [7], but also what is necessary to control the chaos in these systems. Second, we may begin to understand what determines the defect statistics and, in turn, the long-wavelength characteristics, of these systems. Third, if Eq. (1) is found to be valid, then separate, but coupled, equations for the defects and the background might allow a simpler description of the complete system [8, 9]. This description might be further simplified through a Langevin equation approach in which the fluctuating background field is replaced by a noise term [10–12].

We have studied Eq. (1) using a representative defect-mediated spatiotemporally chaotic system, the two-dimensional complex Ginzburg-Landau equation [1]:

$$\partial_t u(\vec{x},t) = u + (1+ic_1)\vec{\nabla}^2 u - (1-ic_3)|u|^2 u, \tag{2}$$

where $u(\vec{x},t)$ is a complex-valued field of size $L\times L$ with periodic boundary conditions, and c_1 and c_3 are real-valued parameters. Eq. (2) is an experimentally relevant amplitude equation universally valid near the onset of a Hopf bifurcation from a stationary homogeneous state to an oscillatory state. It is closely related to equations describing chemical reaction-diffusion systems and excitable media such as heart tissue. For a range of values of the parameters (c_1, c_3), solutions to Eq. (2) exhibit a defect-mediated spatiotemporally chaotic state in which pairs of spirals of opposite topological charge are continually created and annihilated [13, 14].

For a wide range of values of (c_1, c_3) in Eq. (2), we demonstrate for the first time that the complexity D of a defect-mediated spatiotemporally chaotic system is *not* solely due to the defects. In fact, the degrees of freedom can be separated into two sources, suggesting that Eq. (1) is an appropriate description of defect-mediated spatiotemporal chaos. Using a new measure, we show that each defect is associated with 1–2 degees of dynamical freedom, and we provide evidence that the remaining degrees of freedom are due to the underlying phase dynamics. This result suggests that the chaotic dynamics might indeed be modelled using separate, but coupled, equations for the defects and the background phase-turbulent field.

II. MEASURES OF DYNAMICAL BEHAVIOR

We integrated Eq. (2) using a pseudospectral method with time-splitting of the operators, carefully testing for convergence with respect to spatial and temporal resolution and with respect to total integration times. Typically, we used a timestep of $\Delta t = 0.05$ time units, a system size of $L = 64$ or $L = 32$ with 2 Fourier modes (or, equivalently, 2 spatial points) per unit of length, and total integration times of about 10^5 time units. Defects were found by counting the number of crossings of the zero contours of the real and imaginary parts of the field $u(\vec{x}, t)$ in Eq. (2).

The exponential divergence of nearby trajectories in chaotic systems suggests that two realizations, $u(\vec{x}, t_1)$ and $u(\vec{x}, t_2)$, of a solution to Eq. (2) can be regarded as statistically independent when the interval $t_2 - t_1$ is sufficiently large. Then, for intervals of duration ΔT such that ΔT covers many statistically independent realizations of the solution, we expect that the root mean square deviation of quantities that are each averaged over intervals of duration ΔT will converge as $\Delta T^{-1/2}$. This conjecture is supported by Fig. 1(a) showing the convergence of measurements of the average defect density, $n^{(\Delta T)}(t)$ as a function of the duration ΔT over which each measurement is averaged. (Each measurement $n^{(\Delta T)}(t)$ is averaged over the interval $t \le t' \le t + \Delta T$.) The measurements $n^{(\Delta T)}(t)$ converge according to the form

$$\left\langle \left(n^{(\Delta T)}(t) - \left\langle n^{(\Delta T)}(t) \right\rangle_t \right)^2 \right\rangle_t^{1/2} \propto \Delta T^{-1/2},$$

where $\langle\rangle_t$ indicates an ensemble average indexed by the time t for the solution $u(\vec{x}, t)$.

To characterize the dynamics of the chaotic states, we calculated the time-dependent spectrum of finite-time Lyapunov exponents ($\lambda_1^{(\Delta T)}(t) \ge \lambda_2^{(\Delta T)}(t) \ge \cdots$) describing the average rate of divergence during time intervals $t \le t' \le t + \Delta T$ for trajectories in phase space that are initially separated by an infinitesimal amount [15]. The finite-time exponents were obtained by an expensive but widely-used algorithm [16] that involves integrating Eq. (2) together with many copies of the linearization of this equation about the solution $u(\vec{x}, t)$.

In previous work on spatiotemporally chaotic systems, researchers [7, 17–19] have focused on the infinite-time-averaged Lyapunov exponents (and the closely related Lyapunov dimension) which average over the fluctuations in the dynamics. In this work, we utilize the natural fluctuations within the dynamics to extract additional information about the system without additional computational expense. (Because the Lyapunov exponents describe behavior in the linear regime about the solution, a standard method [16] for obtaining the infinite-time exponents is to average the appropriately ordered finite-time Lyapunov exponents.) The fluctuations in the complexity of the dynamics is reflected in changes in the spectrum of finite-time Lyapunov exponents. In analogy to the Kaplan-Yorke conjecture for (infinite-time) Lyapunov exponents [1], we reduce the spectrum to a single quantity by defining a new time-dependent measure of the dynamical complexity, the finite-time dimension $D^{(\Delta T)}(t)$:

$$D^{(\Delta T)}(t) \equiv k^{(\Delta T)}(t) - \left(\sum_{i=1}^{k^{(\Delta T)}(t)} \lambda_i^{(\Delta T)}(t) \right) \left(\lambda_{k^{(\Delta T)}(t)+1}^{(\Delta T)}(t) \right)^{-1},$$

where $k^{(\Delta T)}(t)$ is the largest integer such that $\sum_{i=1}^{k^{(\Delta T)}(t)} \lambda_i^{(\Delta T)}(t) \ge 0$.

Fig. 1(b) suggests that sufficiently separated values of this new measure $D^{(\Delta T)}(t)$ can be regarded as statistically independent. We also note that in the limit $T \to \infty$, $D^{(\Delta T)}(t)$ approaches the (infinite-time) Lyapunov dimension D_L. All results are obtained in the extensive chaos regime for which D_L and $\langle n(t) \rangle_t$ grow linearly with system size L^2.

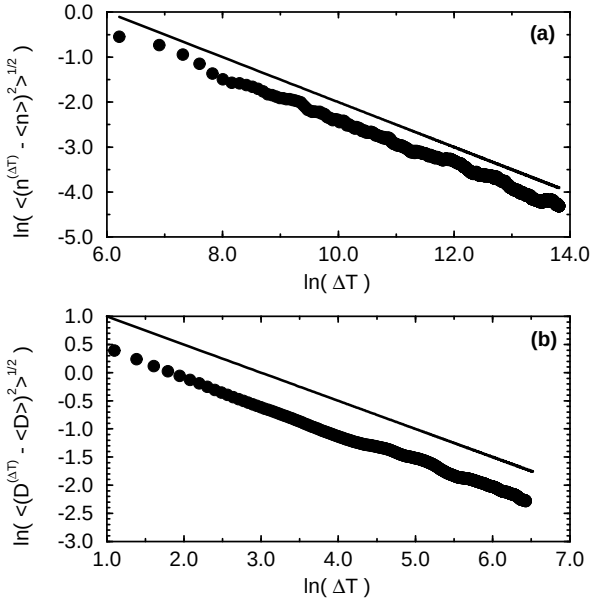

FIG. 1. (a) Convergence of the root mean square deviation of the finite-time defect density $n^{(\Delta T)}(t)/L^2$ as a function of the time interval ΔT. In addition to averages over t, results were averaged over 64 different initial conditions for $(c_1, c_3) = (3.5, 0.90)$ in systems of size 32×32 with $\Delta T = 500$. (b) Convergence of the root mean square deviation of the finite-time dimension $D^{(\Delta T)}(t)$ for a system of size 32×32, $(c_1, c_3) = (3.5, 1.15)$, and $\Delta T = 32$. Solid lines are guides to the $\Delta T^{-1/2}$ power law.

III. THE DIMENSION PER DEFECT

Our new measure, the finite-time dimension $D^{(\Delta T)}(t)$, allows the comparison of fluctuations in the complexity

to fluctuations in the number of defects (for each set of system parameters), effectively separating the degrees of freedom correlated with the defects from the remaining degrees of freedom. Using our calculation of these time-varying quantities, we directly test Eq. (1). For a representative set of the system parameters, ($c_1 = 3.5, c_3 = 1.15$), Fig. 2(a) shows the finite-time dimension $D^{(\Delta T)}(t)$ plotted as a function of the average number of defects $n^{(\Delta T)}(t)$ found *during the same time interval* of duration ΔT. Each point in Fig. 2(a) represents an average of the values of $D^{(\Delta T)}(t)$ for which $n^{(\Delta T)}(t)$ is within a small range of size 0.2 defects. According to Eq. (1), the slope of the fit yields D_d, the average number of degrees of freedom associated with each defect. The average number of degrees of freedom not correlated with the defects, $\langle D_b \rangle_t$ in Eq. (1), is a significant fraction of the the total dimension. (The relatively large contributions of $\langle D_b \rangle_t$ to the total dimension can provide misleading information concerning the dimension per defect if one simply compares the (infinite-time) Lyapunov dimension to the number of defects.) For a wide range of values of finite-time interval ΔT tested (16 time units $\leq \Delta T \leq$ 256 time units), the values of the slope and intercept are approximately constant to within measurement errors, with the range of values of $D^{(\Delta T)}(t)$ and $n^{(\Delta T)}(t)$ decreasing with increasing ΔT. The accuracy at larger values of ΔT is severely restricted by the decrease in the number of measurements and the narrowness of the dimension and defect distributions.

Figures similar to Fig. 2(a) are obtained for a wide range of parameters (c_1, c_3). Fig. 2(b) shows the values of D_d obtained from linear fits of the data for each set of system parameters. We find that D_d decreases slowly as the number of defects increases. We note that a rough extrapolation of the data in Fig. 2(b) toward zero defects suggests an approximate value of $D_d \approx 2$.

Further work (at great computational expense) will be necessary to discern the physical origin of the measured values of D_d. The value of D_d may indicate the average fractal dimension of the trajectories of defects; for example, a value of $D_d = 2$ would be expected if the trajectory of a defect is essentially random in two spatial dimensions. Possible explanations for the decrease in D_d at larger defect densities are correlated behavior between defects and constraint of the defect trajectories due to the proximity of other defects. Evidence of these possibilities might be found in the small amount of negative curvature observed in Fig. 2(a) and similar plots for other parameter values. However, much more data will be needed to measure the curvatures accurately and to assess the impact of these small curvatures on other quantities reported here. The small magnitudes of the curvatures are consistent with analytical and numerical work showing that defects in Eq. (2) are weakly interacting [9].

We are currently investigating these ideas, and we are studying whether similar values of D_d are found in other defect-mediated spatiotemporally chaotic systems.

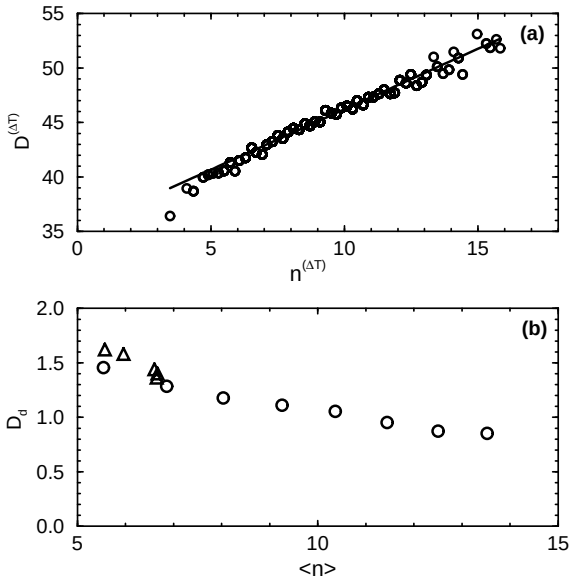

FIG. 2. (a) Finite-time dimension $D^{(\Delta T)}(t)$ vs. the average number of defects $n^{\Delta T}(t)$ during the same interval $\Delta T = 32$ time units for $(c_1, c_3) = (3.5, 1.15)$ in a system of size 32×32. Each point is an average over all measurements with $n^{\Delta T}(t)$ within bins of width 0.2 defects. The solid line is a linear fit with each point weighted by the number of measurements in the respective bin. (b) Values of D_d for various parameters (c_1, c_3). Circles indicate $c_1 = 3.5$ and $0.85 \leq c_3 \leq 1.55$; triangles indicate $c_3 = 0.9$ and $2.5 \leq c_1 \leq 5.0$.

IV. THE PHASE CONTRIBUTION

The non-defect degrees of freedom $\langle D_b \rangle_t$ vary significantly over our range of system parameters, as seen in Fig. 3. We speculate that this "background" contribution is due to an underlying phase turbulence. To elucidate this further, we obtained an estimate of $\langle D_b \rangle_t$ using a phase equation derived in the limit $\nu = (c_1 c_3 - 1) \to 0$ [20]. Upon rescaling, the phase equation can be written in a parameter-less form known as the two-dimensional Kuramoto-Sivashinsky equation:

$$\partial_t \theta(\vec{x}, t) = -\vec{\nabla}^2 \theta - (\vec{\nabla}\theta)^2 - \vec{\nabla}^2 \vec{\nabla}^2 \theta. \qquad (3)$$

The scaling leading to Eq. (3) introduces a factor

$$\alpha = \left(\frac{2}{c_1(c_1 + c_3)} \right)^{1/2} (c_1 c_3 - 1)^{1/2},$$

allowing the computation of a "phase dimension" D_θ of Eq. (2) as a function of (c_1, c_3) and the system area $A_{\rm CGL} = L \times L$, given a *single* measurement of the (infinite-time) dimension $D_{\rm KS}$ of Eq. (3) for a system of size $A_{\rm KS}$ [18]:

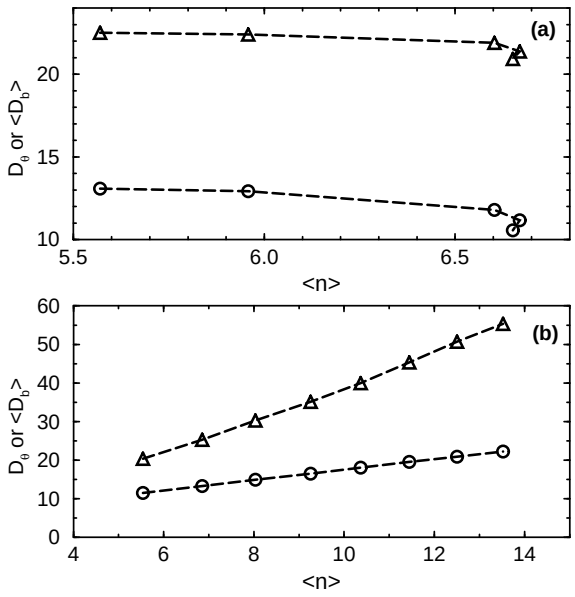

FIG. 3. Background dimension $\langle D_b \rangle_t$ (triangles) and phase dimensions D_θ (circles) for (a) $c_3 = 0.9$ and $2.5 \leq c_1 \leq 5.0$, and (b) $c_1 = 3.5$ and $0.85 \leq c_3 \leq 1.55$.

$$\frac{D_\theta}{A_{\rm CGL}} = \frac{D_{\rm KS}}{A_{\rm KS}} \alpha^2. \tag{4}$$

Remarkably, as seen in Fig. 3, the behavior of the phase dimension D_θ as a function of the average number of defects $\langle n(t) \rangle_t$ is similar to the behavior of the measured average background dimension $\langle D_b \rangle_t$ (although the prediction of Eq. (4) is smaller than the measured values). This is particularly evident in the non-trivial behavior on the right-hand side of Fig. 3(a). This result is particularly surprising since Eq. (3) is derived from an expansion in the small parameter $\nu = (c_1 c_3 - 1) \to 0$, while, for the solutions studied here, $\nu = \mathcal{O}(1)$. Additionally, since the defects are not bound in pairs of opposite topological charge, the phase of the complex field should be globally influenced by the presence of the defects. The effect of the defects on the phase dimension might not be as large as one would naively expect since chaotic lengthscales have been shown to be much shorter than lengthscales corresponding to the phase [7, 18, 19]; however, this effect might account for the increased difference between D_θ and $\langle D_b \rangle_t$ when the system contains more defects, as seen in Fig. 3(b). That similarities remain even in the presence of these effects suggests that the background dimension is closely related to the phase turbulence.

Additional insight might also be gained by studying the solutions to Eq. (3) and the solutions to Eq. (2) for some small values of ν. These solutions are purely phase turbulent cellular patterns [14] with the cells delineated by shocks in the phase field. A cellular pattern also can be found in the defect-turbulent state of Eq. (2) with the defects moving predominantly within the cells. Further work will be required to test whether the number of these cells is related to the background dimension.

V. CONCLUSIONS

Prompted by measurements of the ergodic nature of spatiotemporally chaotic attractors, we have defined a new time-dependent measure, the finite-time dimension. By employing this measure we have found a linear relationship between the degrees of dynamical freedom and the number of defects in the system during the same time interval. These results show that each defect in a defect-mediated spatiotemporal chaotic system is associated with $D_d \approx 1$–2 degrees of freedom. However, a large number of degrees of freedom are not associated with the defects, and we have provided evidence that these degrees of freedom are related to the underlying phase turbulence. Our results yield a deeper understanding of defect-mediated chaos and provide hope that these complicated systems might be reduced to simpler descriptions.

We thank E. Bodenschatz, I. Melnikov, and H. Riecke for valuable discussions. This work was supported by the US National Science Foundation and the Cornell Theory Center.

[1] M. C. Cross and P. C. Hohenberg, Rev. Mod. Phys. **65**, 851 (1993).
[2] Q. Ouyang and J.-M. Flesselles, Nature **379**, 143 (1996).
[3] R. E. Ecke, Y. Hu, R. Mainieri, and G. Ahlers, Science **269**, 1704 (1995).
[4] K. J. Lee, E. C. Cox, and R. E. Goldstein, Phys. Rev. Lett. **76**, 1174 (1996).
[5] F. Melo, P. Umbanhower, and H. L. Swinney, Phys. Rev. Lett. **75**, 3838 (1995).
[6] A. F. M. Maree and A. V. Panfilov, Phys. Rev. Lett. **78**, 1819 (1997).
[7] D. A. Egolf and H. S. Greenside, Nature **369**, 129 (1994).
[8] C. Elphick and E. Meron, Physica D **53**, 385 (1991).
[9] I. S. Aranson, L. Kramer, and A. Weber, Physica D **53**, 376 (1991).
[10] V. Yakhot, Phys. Rev. A **24**, 642 (1981).
[11] S. Zaleski, Physica D **34**, 427 (1989).
[12] G. Grinstein, C. Jayaprakash, and R. Pandit, Physica D **90**, 96 (1996).
[13] P. Coullet, L. Gil, and J. Lega, Phys. Rev. Lett. **62**, 1619 (1989).
[14] H. Chaté and P. Manneville, Physica A **224**, 348 (1996).
[15] E. Ott, *Chaos in Dynamical Systems* (Cambridge U. Press, New York, 1993).
[16] T. S. Parker and L. O. Chua, *Practical Numerical Algorithms for Chaotic Systems* (Springer, New York, 1989).
[17] P. Manneville, in *Liapounov exponents for the Kuramoto-*

Sivashinksy model, Vol. 230 of *Lecture Notes in Physics* (Springer-Verlag, ADDRESS, 1985), pp. 319–326.
[18] D. A. Egolf and H. S. Greenside, Phys. Rev. Lett. **74**, 1751 (1995).
[19] C. S. O'Hern, D. A. Egolf, and H. S. Greenside, Phys. Rev. E **53**, 3374 (1996).
[20] Y. Kuramoto and T. Tsuzuki, Prog. Theo. Phys. **65**, 356 (1976).